Thin Film PZT Multimode Resonant MEMS Temperature Sensor

Wen Sui[1,†*], Tahmid Kaisar[1,†*], Haoran Wang[1], Yihao Wu[1], Jaesung Lee[1], Huikai Xie[2], Philip X.-L. Feng[1,*]

[1]Department of Electrical and Computer Engineering, University of Florida, Gainesville, FL 32611, USA

[2]School of Integrated Circuits and Electronics, Beijing Institute of Technology (BIT), Beijing 100081, China

[*]Emails: wen.sui@ufl.edu, kaisart@ufl.edu, philip.feng@ufl.edu [†]Equally Contributed Authors

***Abstract*—This digest paper reports on the experimental demonstration of an integrated multimode resonant MEMS temperature sensor by exploiting a thin film ceramic PZT multi-frequency piezoelectric micromachined ultrasonic transducers (pMUTs) in the MHz range. The three resonance modes examined (at 1.107, 3.620, 6.778MHz) all exhibit excellent linearity and responsivity to temperature variations in the range of 0 to 211°C, with temperature coefficients of resonance frequency (TC*f*) at ~ -200 to -270ppm/°C for open-loop measurement. We have demonstrated the temperature sensing with real-time tracking of the resonance frequency using a phase-locked loop. We also build a self-sustaining MEMS oscillator and study the closed-loop TC*f* which is smaller than the open-loop TC*f*. We compare the open-loop and closed-loop TC*f*s in both air and vacuum for different type of heaters and find that the TC*f* can be affected by heating method, pressure, and measurement scheme.**

***Keywords*—MEMS; ceramic PZT; temperature sensor; oscillator; phase-locked loop**

I. Introduction

Resonant sensors are frequency output sensors and have become a common solution for sensing many physical parameters such as mass, pressure, temperature, and viscosity. Since the first remote temperature sensors were demonstrated in 1987 based on lithium niobate ($LiNbO_3$) surface acoustic wave (SAW) devices [1], a variety of such devices have been developed and are widely used [2]. Conventionally, piezoelectric crystals such as $LiNbO_3$ or quartz were exploited to fabricate resonant temperature sensors. The high responsivity to temperature in specific crystalline cuts of quartz has enabled sensors with very high resolution (0.001°C) [3]. The drawback, however, is their relatively large size and incompatibility of their fabrication processes with the mainstream silicon microfabrication technology [4]. Microelectromechanical systems (MEMS) technology has been in development over recent decades. Thanks to miniaturization, MEMS devices are ultrasensitive to external perturbations, making them excellent candidates for physical sensors, particularly resonant-mode sensors for physical stimuli and perturbations [5,6].

Toward the emerging industry 4.0 with prevailing internet of things (IoT) and the swarm of trillion sensors perspective, new advances in miniaturized, ultralow-power or self-powering, multifunctional integrated sensors are increasingly demanded [7]. Miniature temperature sensors, in particular, while being ubiquitous and having various existing solutions in conventional methods (*e.g.*, thermistors, diodes, transistors, *etc.*), still face new challenges in emerging applications, such as in smart buildings and industry plants, self-driving vehicles (*e.g.*, monitoring temperature of engine or other critical parts), fire-fighting drones, and medical implants, *etc*. High precision, energy efficiency, and harsh-environment resilience are critical in such scenarios while conventional thermistor/diode options are increasingly unfit. Micromachined thin-film PZT is an excellent platform (with piezoelectric coefficient higher than those of ZnO and AlN) for enabling efficient piezoelectric microsystems on chip [8]. As thin PZT energy harvesters and pMUT have been well known [9], here we demonstrate a thin PZT temperature sensor that we envision can be co-integrated onto the same platform.

II. Device Design and Fabrication

The proposed PZT MEMS devices are fabricated via a simple three-mask process [10]. The key fabrication processes include a temporary bonding of a PZT wafer to a Si wafer, a chemical mechanical polishing (CMP) of ceramic PZT, and a permanent bonding of PZT thin film with an SOI wafer. The 4μm-thick ceramic PZT is first patterned to expose the bottom electrode by wet etching. Next, the top electrode pattern is defined by photolithography and formed by Au sputtering and liftoff process. After that, the cavities are defined by a two-side photolithography and DRIE. A customized heating and temperature sensing stage is utilized to precisely regulate the temperature. Multimode resonances are measured by a network analyzer in the temperature range of 25 to 211°C. We build a bridge circuit with two different devices to null the electrical background, and track the frequency in *real time* using a phase-locked loop (PLL).

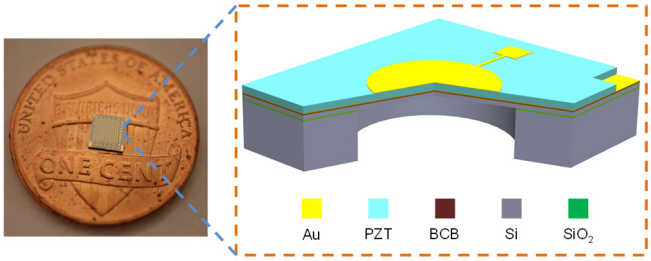

Fig. 1. Optical image of the MEMS chip and the 3D cross-sectional view of the PZT MEMS device.

III. Results and Discussions

A. Temperature-Dependent Multimode Resonances

We first characterize the multimode resonances of circular diaphragm PZT MEMS resonators with diameter of 172μm, at 25°C, by using the network analyzer. Three resonance modes are observed in the range of 1 to 8MHz, f_1

2022 IEEE Sensors | 978-1-6654-8464-0/22/$31.00 ©2022 IEEE | DOI: 10.1109/SENSORS52175.2022.9967330

=1.107MHz, f_2=3.620MHz, f_3=6.778MHz. For fundamental mode, the device has a Q factor of 50.

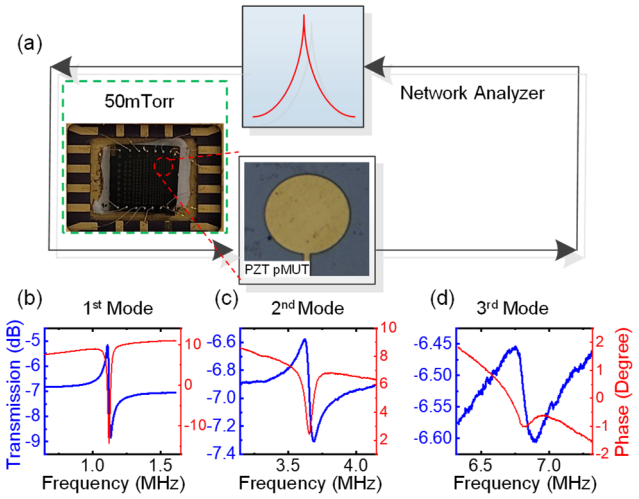

Fig. 2. (a) Illustration of the measurement system. (b)-(d) Measured resonance responses at room temperature from a PZT resonator with diameter of 172μm.

To determine the temperature coefficient of resonance frequency (TCf), we measure these modes in the temperature range of 25 to 211ºC. The MEMS device chip is mounted in a ceramic package and faced the heater. The resonance frequencies of the three modes are recorded, and their TCf values are evaluated by using

$$\mathrm{TC}f = \frac{1}{f}\frac{\Delta f}{\Delta T}, \tag{1}$$

where T is temperature. We find that the resonance frequencies decrease monotonically with increasing temperature (Fig. 3). We plot the frequency shift at different temperatures with respect to its resonance frequency at 25 °C for each of the 3 modes, in which a linear relation between $\Delta f/f$ and T is observed from each mode (Fig. 3b-d). We then extract an average TCf_1 = -193ppm/ºC for the first mode, TCf_2 = -268ppm/ºC for the second mode, and TCf_3 = -255ppm/ºC for the third mode. The linear temperature dependence and TCf values of the PZT MEMS resonator can be directly exploited for on-chip temperature sensing.

B. Real-Time Tracking of Resonance with PLL

To demonstrate resonant temperature sensing with real-time tracking of the resonance frequency, we first build a balanced bridge circuit with two devices on the same chip. By carefully adjusting the bridge circuit [11], the electrical background rising from parasitic effects and impedance mismatch can be minimized, enabling higher signal-to-background ratios [11]. We then track the resonance of the first mode with PLL while applying heating pulses (Fig. 4). The PZT MEMS devices respond rapidly to the changes in temperature. However, it takes tens of minutes for the frequency to be stabilized. From thermal circuit model, we obtain the thermal time constant value of 8 min. This could be attributed to at least two factors. One effect may be caused by the slow heating process of the ceramic heater. Another may result from the slow heat transfer from the heater to the MEMS devices.

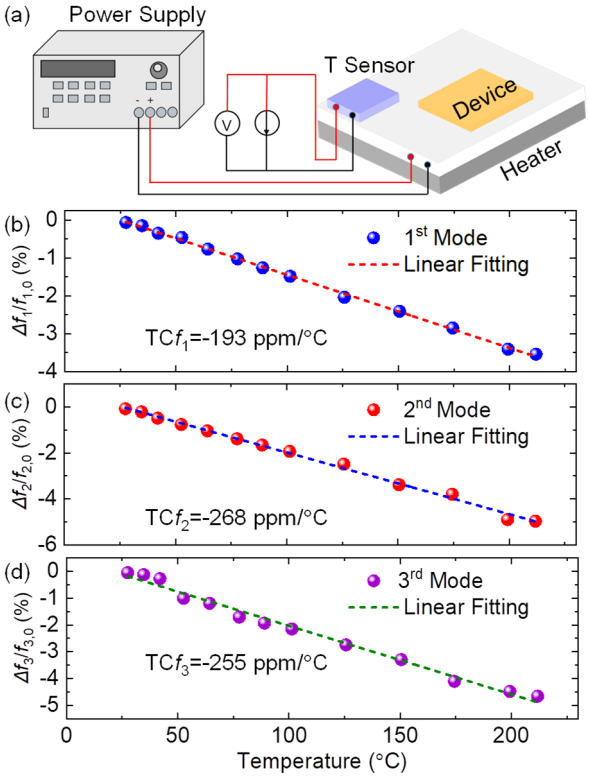

Fig. 3. (a) Illustration of temperature-controlled heating stage. (b)-(d) Fractional frequency shift of the 3 modes with varying temperature from 25°C up to 211°C.

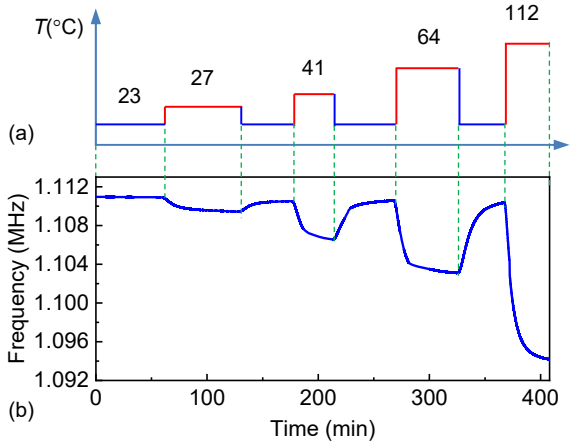

Fig. 4. Real-time frequency tracking of the 1st mode to heating pulses attained in the closed-loop measurement.

C. Self-Sustaining MEMS Oscillator

We then build a self-sustaining MEMS oscillator using the PZT MEMS resonator. We first perform open-loop measurement to calibrate on meeting the Barkhausen criteria, with the overall open-loop gain slightly greater than 0dB near the resonance frequency and the overall phase shift to be $2n\pi$, where n is an integer. After satisfying the Barkhausen criteria, we close the loop and characterize the stable self-oscillation both in frequency domain and time domain (Fig. 5a-b). Then we characterize the oscillator's performance by measuring its frequency stability. From the time-domain tracked frequency data trace, we calculate the Allan deviation (Fig. 5d) from [11]

$$\sigma_A(\tau_A) = \left[\frac{1}{2(N-1)}\sum_{i=1}^{N-1}\left(\frac{\overline{f_{i+1}}-\overline{f_i}}{f_{osc}}\right)^2\right]^{1/2}, \qquad (2)$$

where $\overline{f_i}$ is the measured average frequency in the i-th discrete time interval of τ_A. The Allan deviation data gives us the short-term frequency stability $\sigma_A \approx 2\times10^{-7}$ at averaging time $\tau_A < 5$s, and long-term frequency stability $\sigma_A \approx 1\times10^{-6}$ at $\tau_A = 1000$s. We then examine the phase noise behavior using the phase noise module in a spectrum analyzer. In the phase noise plot, we see two main regions. Phase noise decreases in 100Hz–10kHz range, following a $1/f^2$ power law, suggesting it is dominated by thermal noise. Phase noise flattens out beyond 10kHz (Fig. 5c).

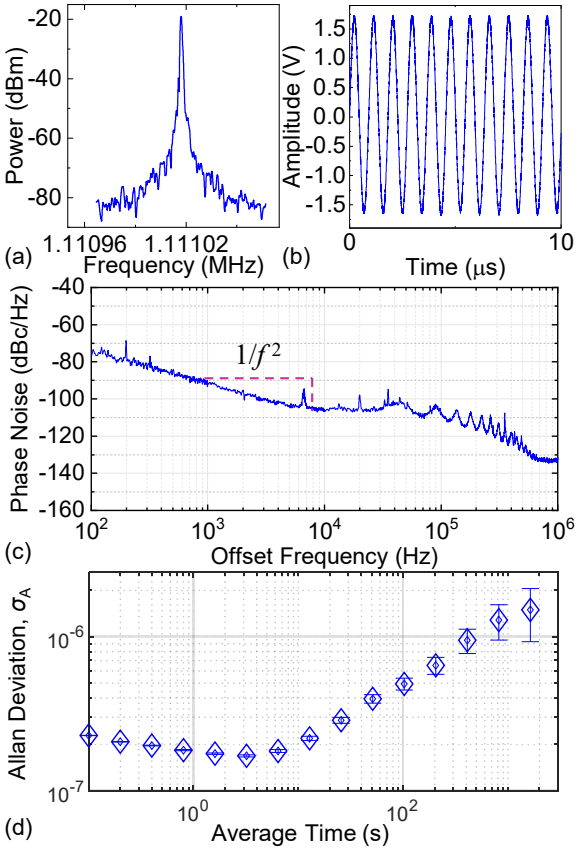

Fig. 5. Self-sustaining MEMS oscillator characteristics from measurement. (a) Oscillator output spectrum. (b) Time-domain waveform. (c) Phase noise. (d) Allan deviation.

D. Closed-Loop TC*f*

To further explore the temperature-dependent resonance of the PZT MEMS device, we have done closed-loop TC*f* measurement on the self-sustaining oscillator in both air and vacuum. We gradually increase the heater voltage from 0 to 9V (Fig. 6a). The resistance of the commercial resistive temperature sensor increases from 109Ω to 150Ω, corresponding to the change of temperature from 25°C to 132°C. Fig. 6b shows the response of frequency variation versus time. To extract the TC*f*, we take the temperature and frequency values after both are stabilized. As shown in Fig. 6c, we obtain $TCf_{1,osc}$ = -88ppm/°C with ceramic heater in air, which is much smaller than TCf_1 measured in open loop. Such difference in TC*f* may be related to the response of the feedback loop circuit of the self-sustaining oscillator.

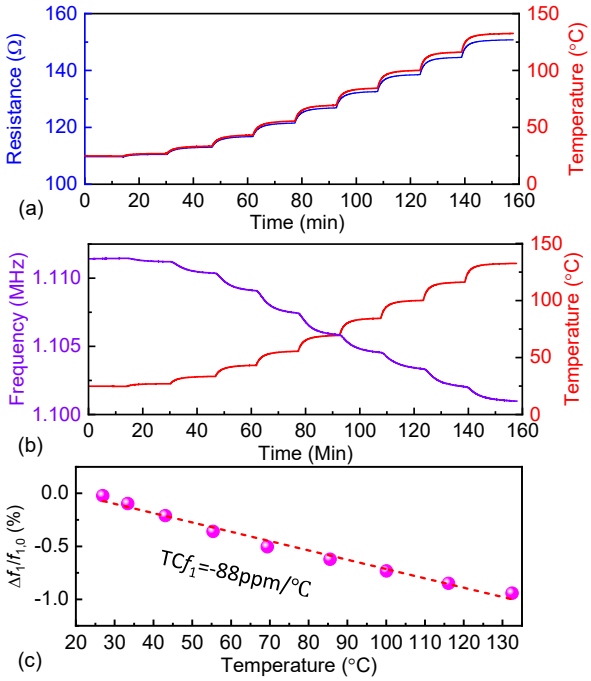

Fig. 6. Closed-loop TC*f* measured with ceramic heater. (a) Temperature readout from a resistive temperature sensor. (b) Real-time tracking of the resonance frequency of the self-sustaining oscillator. (c) Fractional frequency shift ($\Delta f_1/f_{1,0}$) with varying temperature, where reference frequency $f_{1,0}$ is the frequency measured at room temperature. The averaged TC*f* is obtained by linear fitting of the $\Delta f_1/f_{1,0}$ versus temperature plot.

TABLE I SUMMARY OF *TCf* MEASURED FROM PZT MEMS DEVICES

Modality	Heater	Pressure	Temperature [°C]	TC*f* [ppm/°C]
Resonator	Ceramic	Air	25 to 211	-193
Resonator	Peltier[a]	50mTorr	0 to 125	-125
Oscillator	Ceramic	Air	25 to 132	-88
Oscillator	Peltier[a]	50mTorr	0 to 125	-38

[a] Measurement data plots using the Peltier heater are not shown here due to limited space.

Table 1 summarizes the TC*f* values measured in different scenarios, from which we observe that the TC*f* can be affected by heating method, pressure, and measurement scheme or modality. The mechanisms of such TC*f* variations require further investigation.

IV. CONCLUSIONS

We have experimentally demonstrated an integrated multimode resonant PZT MEMS temperature sensor. All the three resonance modes exhibit excellent linearity and responsivity to temperature variations from 0 to 211ºC, with TC*f* ~ -200 to -270ppm/ºC for open-loop measurement. We have demonstrated temperature sensing with real-time tracking of the resonance frequency using a phase-locked loop (PLL). We have also measured the closed-loop TC*f* based on a self-sustaining PZT MEMS oscillator. The results indicate that the measured TC*f* can be affected by heating method, vacuum level, and measurement scheme.

V. ACKNOWLEDGEMENTS

The authors are grateful to the support from the National Science Foundation (NSF) via the CISE CCF-FET Program (Grant No. CCF-2103091), the National Institutes of Health (NIH) via the Grant R01EB020601, and the Margaret A. Ross Fellowship (W. Sui) from ECE, University of Florida.

REFERENCES

[1] X. Q. Bao, W. Burkhard, V. V. Varadan, and V. K. Varadan, "SAW temperature sensor and remote reading system," in *Proc. IEEE Int. Ultrason. Symp.*, Dec. 1987, pp. 583-586.

[2] S. Ren, W. Yuan, D. Qiao, J. Deng, and X. Sun, "A micromachined pressure sensor with integrated resonator operating at atmospheric pressure," *Sensors*, vol. 13, no. 12, pp. 17006-17024, 2013.

[3] T. Ueda, K. Fusao, T. Iino, and D. Yamazaki, "Temperature sensor using quartz tuning fork resonator," in *Proc. IEEE Intl. Freq. Cont. Symp.*, May 1986, pp. 224-229.

[4] H. Fatemi, M. J. Modarres-Zadeh, and R. Abdolvand, "Passive wireless temperature sensing with piezoelectric MEMS resonators," in *Proc. IEEE 28th Int. Conf. Micro Electro Mech. Syst. (MEMS)*, Jan. 2015, pp. 909–912.

[5] W. Sui, X.-Q. Zheng, J.-T. Lin, B. W. Alphenaar, and P. X.-L. Feng, "Thermal response and TC*f* of GaN/AlN heterostructure multimode micro string resonators from -10°C up to 325°C," *J. Microelectromech. Syst.*, vol. 30, no. 4, pp. 521-529, 2021.

[6] W. Sui, H. Wang, J. Lee, A. Qamar, M. Rais-Zadeh, and P. X.-L. Feng, "AlScN-on-SiC thin film micromachined resonant transducers operating in high temperature environment up to 600°C," *Adv. Funct. Mater.*, art. no. 2202204, 2022.

[7] P. Mpeis, T. Roussel, M. Kumar, C. Costa, C. L. Denis, D. Capot-Ray, and D. Zeinalipour-Yazti, "The anyplace 4.0 IoT localization architecture, " in *Proc. 2020 21st IEEE Int. Conf. Mob. Data Mgmt. (MDM)*, Aug. 2020, pp. 218-225.

[8] Y. Qiu, J. V. Gigliotti, M. Wallace, F. Griggio, C. E. M. Demore, S. Cochran, and S. Trolier-McKinstry, "Piezoelectric micromachined ultrasound transducer (PMUT) arrays for integrated sensing, actuation and imaging," *Sensors*, vol. 15, pp. 8020-8041, 2015.

[9] A. Khan, Z. Abas, H. S. Kim, and I. Oh, "Piezoelectric thin films: an integrated review of transducers and energy harvesting," *Smart Mater. Struct.* vol. 25, art. no. 053002, 2016.

[10] H. Wang, P. X.-L. Feng, and H. Xie, "A high-density and dual-frequency PMUT array based on thin ceramic PZT for endoscopic photoacoustic imaging," in *Proc. IEEE 34th Int. Conf. Micro Electro Mech. Syst. (MEMS)*, Jan. 2021, pp. 891-894.

[11] X. L. Feng, C. J. White, A. Hajimiri, and M. L. Roukes, "A self-sustaining ultrahigh-frequency nanoelectromechanical oscillator," *Nature Nanotechnology*, vol. 3, no. 6, pp. 342-346, 2008.